Description of the lowest-energy surface of the CH+O system: Interpolation of *ab initio* configuration-interaction total energies by a tight-binding Hamiltonian

N. C. Bacalis* and A. Metropoulos
Theoretical and Physical Chemistry Institute, National Hellenic Research Foundation, Vasileos Constantinou 48, GR-116 35 Athens, Greece

D. A. Papaconstantopoulos
Center for Computational Materials Science, Naval Research Laboratory, Washington, D.C. 20375-5345, USA
(Received 7 October 2004; published 11 February 2005)

It is demonstrated that the potential-energy surface and the lowest-energy path for a polyatomic molecule (applied to the CH+O system) is accurately calculated via *bond-length-dependent* tight-binding Hamiltonian, fitted to *ab initio* configuration-interaction (CI) total energies. This Hamiltonian not only reproduces the CI energies accurately and efficiently, but also effectively recognizes and identifies CI energy values that may erroneously converge to excited states. The resulting normal mode frequencies are in very good agreement with experiment.

DOI: 10.1103/PhysRevA.71.022707 PACS number(s): 34.20.−b

I. INTRODUCTION

A. The question

The determination of the reaction path in a chemical reaction needs detailed knowledge of the pertinent potential energy surface (PES) (diabatic or adiabatic). In practice this is a formidable task because (i) the PES is a multidimensional surface, impossible to be *ab initio* calculated at every point in the degrees of freedom (DOF) space, and interpolation is necessary (the most accurate known detailed multidimensional PES is that of H_3 interpolated from 71 969 *ab initio* DOF points [1]); (ii) because the standard *ab initio* calculations of the many-electron problem in the Born-Oppenheimer approximation, based on the variational principle [accurate *ab initio* configuration-interaction (CI) calculations], yield only adiabatic curves and, more importantly, being iterative, sometimes converge to undesirable states ([2]; also cf. below). Yet such calculations may be prohibitively computer time consuming. For the ground state, the time problem is already traditionally overcome via density functional theory (DFT) [3], which self-consistently approximates the many-electron problem by a one-electron problem. However, DFT calculations sometimes fail to describe experimentally observed features of the PES [4]. Thus, the accurate CI calculations are more or less indispensable, even if performed in a rather limited, but representative, set of molecular geometries. There are quite a few general methods for fitting *ab initio* potentials for diatomic or small polyatomic molecules, based either on piecewise cubic spline fits or fits to functional forms such as Morse, extended Rydberg, LEPS (London-Eyring-Polanyi-Sato), diatomics in molecules (DIM), and many-body expansions, as described with references for details in Ref. [5]. The analytically parametrized interpolation schemes become very complicated for polyatomic species, and they are not able to recognize and identify any inadvertent wrong CI convergence [2], which may escape attention. Therefore, a reliable interpolation scheme for the pertinent PES of polyatomic species, based on CI calculations, also able to identify any error in the CI database or, in general, in any fitting database, is desirable.

B. The purpose

It is shown that such an interpolation scheme is possible, based on a spin-polarized [6] bond-length-dependent [7] Slater-Koster (SK) parametrization [8] of *ab initio* CI total energies [9]. We present this method [previously unreported for (spin-polarized) molecules], and as a demonstration, we apply it to a triatomic molecule of chemical kinetics interest, HCO [which is an intermediate radical in the generation of a primary ion during hydrocarbon combustion: $O(^3P)+CH(X\,^2\Pi$ and/or $a\,^4\Sigma^-) \rightarrow [HCO]^*(^2A') \rightarrow HCO^+ + e^-$]. The reaction of H+CO—i.e., H in the vicinity of CO—has been thoroughly studied in the past. On the other hand, the reaction of $O(^3P)+CH(X\,^2\Pi, a\,^1\Sigma^-)$—i.e., O in the vicinity of CH—is known experimentally [10] to generate the HCO^+ cation via autoionization of some state (or states) of the intermediate HCO radical upon interaction with some vibrational level of the ion. The first step toward understanding such interactions is the construction of the PES of the states with low (or without) barrier, through which a reaction at the experimental temperature can proceed. Such a state (without a barrier) is the $HCO(X\,A')$ neutral intermediate state [11]. Thus, in order to *test* the interpolation scheme on a *molecular system*, this state is used in this work.

The interpolation is then applied: (i) to the prediction of the lowest-energy path (in $^2A'$ symmetry) while O approaches the vicinity of HC, (ii) to the generation of a more

*Corresponding author. FAX: +30(210)7273794. Electronic address: nbacalis@eie.gr

accurate PES at optimum C-H distances (not just at constant C-H distance), and (iii) to the computation of the potential energy curvatures at equilibrium and of the concomitant normal-mode frequencies, which are in satisfactory agreement with experiment.

C. The procedure

First several (724, contrary to 71 969 of H_3 [1]) accurate CI total energies, based on multiconfiguration self-consistent field (MCSCF) orbitals, are calculated at selected geometries of the H,C,O atoms in the A' symmetry of the Cs group. Typically, e.g., for a cubic spline fit, for a triatomic PES at least $10^{3N-6}=10^3$ CI points would be needed. For H+CO, Bowman *et al.* [12] used about 2000 *ab initio* points. With the present interpolation scheme no more than 508 CI points were needed, the remaining serving to check the quality of the fit. For the fit a nonorthogonal spin-polarized tight-binding (TB) Hamiltonian is formed; the matrix elements of the TB Hamiltonian (and of the overlap matrix) are expressed as *functions* of the bond direction, according to the SK scheme [8], and of the bond length, according to the Naval Research Laboratory (NRL) technique [7]: i.e., these *functions* are generally polynomials of the interatomic distance, within exponential envelopes, the coefficients and the exponents being varied as parameters. For two adiabatic states near some (avoided) crossing the TB Hamiltonian naturally produces two diabatic PES's in nearby extrapolation and predicts to which diabatic PES, ground state or excited, nearby CI energies belong. Among these, after identification, the appropriate ones can be used to extend the fit beyond the (avoided) crossings, around which two sets of parameters are needed, one for each branch of the PES. If it happens, as with HCO, that the ground- and excited-state energies beyond the crossing lie close to each other, comparably to the fitting accuracy, the adiabatic PES can be fitted as well, with comparable accuracy.

After the fit, in the TB Hamiltonian scheme, by using at each point of the DOF space either the desired diabatic or the lowest-lying (adiabatic) TB-fitted PES, the diabatic or the adiabatic lowest-energy *path* can be found (without any more lengthy *ab initio* calculations): For each value of a desired degree of freedom (in our case for each C-O distance) the energy minimum is searched [13] in the space of the remaining degrees of freedom (C-H distance and H-C-O angle). Similarly, by optimizing the energy with respect to all other degrees of freedom except two, an optimal energy *surface* can be found and so on. An important feature of the parametrized TB Hamiltonian is that, by using it, any property can be trivially computed, contrary to conventional analytically parametrized interpolation schemes. Here we compute the normal modes.

II. THE CALCULATION

A. Methodology

For the CI energies the correlation consistent aug-cc-pVTZ basis set was used [14,15] in conjunction with the complete active space self-consistent field (CASSCF)+1+2 multireference CI method (MRCI) employed in the MOLPRO package [9] (the four electrons in the 1*s* orbitals of C and O were unexcited). The method of calculation is described in more detail in Ref. [11]. The CASSCF calculations were state averaged, and the active space was limited to the 9 valence orbitals among which the remaining 11 electrons were distributed. In the subsequent MRCI calculations the uncontracted configurations were around 50×10^6, internally contracted to about 1×10^6. Calculations between C-O distances of 1.7 and 6 bohrs were performed for several H-C-O angles between 50° and 180° and several C-H distances between 1.7 and 4.5 bohrs, most around the C-H equilibrium distance, 2.1 bohrs. The three lowest roots of the secular equation were computed, increasing (compared to one root) the number of useful configurations, therefore, increasing the accuracy of the calculation and guarding against root flipping. By an analytic gradient optimization at the MCSCF level, an approximate (MCSCF) equilibrium geometry was found at the DOF space point $(\tilde{r}_{HC},\tilde{r}_{CO},\tilde{\theta}_{H\text{-}C\text{-}O})=(2.12\text{ a.u.},2.2\text{ a.u.},126°)$. In order to determine a physically reasonable interpolating TB Hamiltonian, the fit must be guided by choosing points (to be fitted) that belong to the correct diabatic branch of the PES. Because it is not evident whether the aforementioned points are beyond any avoided crossing, where the role of the ground and excited states would be interchanged, first several DOF points near equilibrium were obtained. This first step of the procedure is essential. It is achieved by employing a generalization [16] of the three-dimensional sphere to the generally multidimensional (in this case also three-dimensional) DOF space: $x_i=(r_i/\tilde{r}_i-1)$, $i=\{\mathrm{HC},\mathrm{CO}\}$, $x_3=(\theta/\tilde{\theta}-1)$, which are the dimensionless relative distances from the equilibrium DOF point; generally for n degrees of freedom, points belonging to a n-dimensional (hyper)sphere of radius r and center $(\tilde{x}_i, i=1,\ldots,n)$ are obtained by

$$
\begin{aligned}
x_n-\tilde{x}_n &= r\cos\theta_n,\\
x_{n-1}-\tilde{x}_{n-1} &= r\sin\theta_n\cos\theta_{n-1},\\
&\cdots\\
x_1-\tilde{x}_1 &= r\sin\theta_n\sin\theta_{n-1}\cdots\cos\theta_1,
\end{aligned}
\tag{1}
$$

an obvious extension of a three-dimensional spherical surface [16]. Here the first $\theta_1=0$ or 180°, the two points of a "one-dimensional sphere," and the other $0<\theta_i<180°$ are the "azimuthal" hypersphere angles (incidentally, a *variable-dimensional* do-loop code was invented, needed to treat any larger molecule). Thus, first, points with small r were fitted, and gradually the fit was extended to more remote DOF points (many of which were actually also predicted by the preceding fits).

B. The NRL bond-length-dependent TB Hamiltonian parametrization

The formalism of the NRL bond-length-dependent TB parametrization is described in detail in Ref. [7]; here an essen-

tial summary and necessary extensions are only presented.

1. The underlying idea

At each molecular geometry, the total CI energy can be written as

$$E[n(\vec{r})] = \sum_{i;s=1,2} f\left(\frac{\mu - \epsilon_{i\,s}}{T}\right)\epsilon_{i\,s} + F[n(\vec{r})]$$

$$\equiv \sum_{i;s=1,2} f\left(\frac{\mu' - \epsilon'_{i\,s}}{T}\right)\epsilon'_{i\,s}, \qquad (2)$$

where [17] $f(x)=1/(1+e^x)$ is the Fermi function with a small tail ($T=0.005$ mRy), $\epsilon_{i\,s}$ are the SCF orbital energies, $n(\vec{r})$ is the electron density, $F[n(\vec{r})]$ represents the rest of the energy—i.e., Coulomb, core, exchange, and correlation energy—and

$$\epsilon'_{i\,s} = \epsilon_{i\,s} + V_0, \quad \mu' = \mu + V_0, \quad V_0 = F[n(\vec{r})]/N_e, \qquad (3)$$

with $N_e=\Sigma_{i;\,s=1,2} f((\mu-\epsilon_{i\,s})/T)$ being the number of electrons, from which the highest occupied energy level μ is determined, i counts the states, and $s=1,2$ counts the spin. In other words, due to the simple observation that $\Sigma_{i,s} f\{(\mu-\epsilon_{i,s})/T\}\ (\epsilon_{i,s}+V_0)=\Sigma_{i,s} f\{[(\mu+V_0)-(\epsilon_{i,s}+V_0)]/T\}\ (\epsilon_{i,s}+V_0)$, the total CI energy at a specific molecular geometry (DOF point) can be rigorously, without approximation, rewritten as the sum of *appropriately uniformly shifted* energies (of fictitious occupied orbitals).

For a *single-molecular geometry* a TB description could fit $\epsilon'_{i\,s}$s as eigenvalues of the generalized eigenvalue problem $(\mathbf{H}-\mathbf{S}\epsilon'_{i\,s})\psi_{i\,s}=0$, $\mathbf{H}$ being the TB Hamiltonian and $\mathbf{S}$ the overlap matrix, under the assumption that these matrices are represented in an atomic s and p (and in general d) orbital basis $\{\phi_a\}$. Under this assumption the matrix elements would be parametrized according to the two-center SK scheme [7], where a nonorthogonal TB calculation would need diagonal on-site and off-diagonal hopping and overlap matrix element parameters: In this scheme the three-center integrals $\langle\psi(\mathbf{r}-\mathbf{a})|V(\mathbf{r}-\mathbf{b})|\psi'(\mathbf{r}-\mathbf{c})\rangle$, as well as $\langle\psi(\mathbf{r}-\mathbf{a})|V(\mathbf{r}-\mathbf{b})|\psi'(\mathbf{r}-\mathbf{a})\rangle$ are omitted, while the on-site and the hopping matrix element parameters are formed by integrals of the type $\langle\psi(\mathbf{r}-\mathbf{a})|V(\mathbf{r}-\mathbf{a})|\psi'(\mathbf{r}-\mathbf{a})\rangle$ and $\langle\psi(\mathbf{r}-\mathbf{a})|V(\mathbf{r}-\mathbf{a})|\psi'(\mathbf{r}-\mathbf{b})\rangle$, respectively [7]. *If the energies were not shifted by V_0, then the two-electron integrals, due to the term $F[n(\vec{r})]$ in Eq. (2), would have to be parametrized as well*, either directly or within DFT. With the shift, this is rigorously avoided.

For *each geometry*, if the usual complete neglect of differential overlap (CNDO) assumptions [18,19] were imposed [i.e., (i) use of orthogonal atomic orbitals or (ii) neglect of their overlap integrals, (iii) neglect of the differential overlap in all two-electron integrals while (iv) reducing the remaining Coulomb-type integrals to one value per atom pair, also (v) neglect of the off-diagonal electronic interaction with neighboring cores while (vi) reducing the diagonal to a single value per atom pair, and (vii) assuming that the off-diagonal core matrix elements were proportional to the corresponding overlap integrals], then this scheme would reduce to the usual CNDO approximation; and if, further, the extended Hückel assumptions [19,20] were imposed [i.e., (viii) to replace the remaining on-site matrix elements by the valence state ionization potential while assuming that the remaining off diagonal matrix elements were (ix) proportional to the mean value of the constituent diagonal and (x) proportional to the corresponding overlap integrals], then the NRL-TB scheme would reduce to the extended Hückel approximation. However, here no special assumptions are made, all matrix elements are maintained in the fit, and the uniform shift (*different for each geometry*) ensures the exact CI energies. It is important that the constant V_0 is different for each geometrical structure of the CI database. It should also be stressed that the shift is done to the first-principles CI database before we proceed with the fit that will generate the TB Hamiltonian.

2. Bond-length dependence

The next step is to use a least-squares procedure to fit this shifted CI database with the shifted eigenvalues $\epsilon'_{i\,s}$ to our TB Hamiltonian, which, needless to say, if it were different for each geometry, would be useless for the construction of the PES; instead, *common* parameters are needed that would reproduce the known shifted energies and their sums for *all* sample molecular geometries, as well as at any interpolated DOF point. Indeed, the matrix element parameters, being functions of the bond angles [8], may also be expressed *geometry independently in terms of functions of the internuclear distances*: If there are several types of atoms $\{A,B,C,\ldots\}$ with N_A atoms of type A $\{A_i, i=1,\ldots N_A\}$, etc., then in a spin-polarized structure the on-site matrix elements are expressed as

$$h_{A_i ls} = b^{(0)}_{AAls} + \sum_{B\in\{A,B,C\ldots\}}\sum_{n=1}^{3} b^{(n)}_{ABls}\varrho^{2n/3}_{A_i Bs}, \quad l=s,p,d, \qquad (4)$$

where

$$\varrho_{A_i Bs} = \sum_{j=1}^{N_B} e^{-\lambda^2_{Bs}R_{A_iB_j}} f\left(\frac{R_{A_iB_j}-R_0}{r_c}\right) \qquad (5)$$

is a generalized pair potential ("density"); here $f(x)=1/(1+e^x)$ is a cutoff function [21] with $R_0=15$ bohr, $r_c=0.5$ bohr. $R_{A_iB_j}$ is the internuclear distance between atoms A_i and B_j, while λ_{As}, depending on the atom type, and $b^{(n)}_{ABls}$ are the on-site NRL bond-length-dependent parametric coefficients (BLDP's) (Tables I–III).

The hopping parameters are of the form

$$P_\gamma(R) = \left(\sum_{n=0}^{2} c^{(n)}_\gamma R^n\right) e^{-g^2_\gamma R} f\left(\frac{R-R_0}{r_c}\right), \qquad (6)$$

where γ indicates the type of interaction (i.e., $ss\sigma$, $sp\sigma$, $pp\sigma$, $pp\pi$, $ps\sigma,\ldots,dd\delta$). The NRL BLDP's are $c^{(n)}_\gamma$ and g_γ (Tables IV–VI). R is the interatomic distance between atoms A and B, and R_0 and r_c are as in Eq. (5).

A similar formula, as originally employed in the NRL-TB code, could be used also for the overlap parameters $S_{ll'\mu}(R)$, but this, for unfitted geometries, might violate the necessary conditions

TABLE I. NRL coefficients of on H-site TB Hamiltonian matrix elements in Eq. (4), in appropriate a.u.: The matrix element is measured in hartree and the distance in bohr; therefore, the NRL parameters $b^{(k)}$ are measured in hartree, and λ in bohr$^{-1/2}$. The first numerical column refers to spin up and the second to spin down.

λ_H	1.0016	1.1216
$b^{(0)}_{HHs}$	1.4191	1.9785
$b^{(1)}_{HHs}$	0.0000	0.0000
$b^{(2)}_{HHs}$	0.0000	0.0000
$b^{(3)}_{HHs}$	0.0000	0.0000
$b^{(1)}_{HCs}$	−9.1049	0.42447
$b^{(2)}_{HCs}$	197.70	22.965
$b^{(3)}_{HCs}$	−675.11	−32.554
$b^{(1)}_{HOs}$	−13.899	1.0108
$b^{(2)}_{HOs}$	47.769	−4.7637
$b^{(3)}_{HOs}$	−74.244	7.5086

$$\{|S_{ll'\mu}(R)| < 1,\ R > 0\}, \quad S_{ll'\mu}(0) = \delta_{ll'}, \tag{7}$$

which are important for molecules. Here, we ensure these conditions by special care: Starting from the 1*s* hydrogenlike overlap integral $\langle 1s(\mathbf{r})|1s(\mathbf{r}-\mathbf{R})\rangle = (1+R+R^2/3)e^{-R}$, we employ, for dissimilar atoms, a parametrization of the form

$$y(g;R) = [1 + (R/g^2) + (R/g^2)^2/3]e^{-R/g^2},$$

$$f(b,c,g;R) = by(g;R)^2 + cy(g;R),$$

$$S_{ll'\mu}(R) = \tanh[-af(b,c,g;R)]f\left(\frac{R-R_0}{r_c}\right), \tag{8}$$

where $|S_{ll'\mu}(R)| < 1$, and, for similar atoms,

$$y(g;R) = [1 + (R/g^2) + (R/g^2)^2/3]e^{-R/g^2},$$

$$f(b,g;R) = by(g;R)^2 + (1-b)y(g;R),$$

$$v(c;R) = [1 + (R/c^2) + (R/c^2)^2/3]e^{-R/c^2},$$

$$S_{ll'\mu}(R) = \{[1 - v(c;R)]\tanh[-af(b,g;R)] + v(c;R)\delta_{ll'}\}f\left(\frac{R-R_0}{r_c}\right); \tag{9}$$

then, necessarily, conditions (7) are obeyed. Similar formulas are used for all $l=s,p,d$. The BLDP parametric coefficients are $\{a,b,c,g\}$ (Tables VII–IX).

3. Approximations

The standard NRL parameters allow for *s*, *p*, and *d* matrix elements (although, in the case of HC-O, fitting with *s* and *p* matrix elements was proven sufficient). Within the context of the NRL code [7], which can treat also solids (for which it was originally written), the molecule was treated as a base to a large cubic lattice unit cell (lattice constant=100 a.u.), ensuring a vanishing interaction between atoms in neighboring cells. Thus, the PES was described in terms of NRL BLDP's for each spin polarization of the following kinds: On-site [in Eqs. (4) and (5)]: *s*: H, C, O, (H depending on C), (C on H), (H on O), (O on H), (C on O), and (O on C); *p*: C, O, (C on H), (O on H), (C on O), and (O on C). Hopping and overlap parameters [in Eqs. (6), (8), and (9)]: $ss\sigma$: H-C, H-O, C-O; $sp\sigma$: H-C, H-O, C-O, and O-C (denoted as $ps\sigma$); $pp\sigma$ and $pp\pi$: C-O. For HCO, since similar atoms are well separated, the H-H, C-C, and O-O parameters vanish. We fitted 508 CI points and we checked the resulting PES against 216 more CI energies not included in the fit. The error was less than 10^{-3} a.u.$\approx$0.6 kcal/mol. To ensure obtaining physically meaningful TB parameters, for a very limited number of molecular geometries the Hamiltonian eigenvalues were also fitted, while the total energy was fitted for all 508 structures.

TABLE II. NRL coefficients of on C-site TB Hamiltonian matrix elements in Eq. (4) (in a.u., as in Table I). The first column refers to spin up and the second to spin down.

λ_C	1.1994	0.62579
$b^{(0)}_{CCs}$	0.41913	0.74891
$b^{(1)}_{CCs}$	0.0000	0.0000
$b^{(2)}_{CCs}$	0.0000	0.0000
$b^{(3)}_{CCs}$	0.0000	0.0000
$b^{(0)}_{CCp}$	0.28771	0.09461
$b^{(1)}_{CCp}$	0.0000	0.0000
$b^{(2)}_{CCp}$	0.0000	0.0000
$b^{(3)}_{CCp}$	0.0000	0.0000
$b^{(1)}_{CHs}$	−1.0827	−12.931
$b^{(2)}_{CHs}$	−4.5710	68.434
$b^{(3)}_{CHs}$	0.81620	−81.019
$b^{(1)}_{CHp}$	3.3728	4.4257
$b^{(2)}_{CHp}$	−25.133	−49.575
$b^{(3)}_{CHp}$	51.719	140.68
$b^{(1)}_{COs}$	0.30836	−0.53199
$b^{(2)}_{COs}$	−2.7725	−0.50810
$b^{(3)}_{COs}$	7.2151	1.5903
$b^{(2)}_{COp}$	−0.62615	0.00528
$b^{(1)}_{COp}$	4.7385	−0.40085
$b^{(3)}_{COp}$	−0.36663	−0.71917

TABLE III. NRL coefficients of on O-site TB Hamiltonian matrix elements in Eq. (4) (in a.u., as in Table I). The first column refers to spin up and the second to spin down.

λ_O	0.86813	0.48862
$b_{OOs}^{(0)}$	1.8033	0.16652
$b_{OOs}^{(1)}$	0.0000	0.0000
$b_{OOs}^{(2)}$	0.0000	0.0000
$b_{OOs}^{(3)}$	0.0000	0.0000
$b_{OOp}^{(0)}$	0.17844	0.19883
$b_{OOp}^{(1)}$	0.0000	0.0000
$b_{OOp}^{(2)}$	0.0000	0.0000
$b_{OOp}^{(3)}$	0.0000	0.0000
$b_{OHs}^{(1)}$	−3.7292	2.6474
$b_{OHs}^{(2)}$	20.399	−35.242
$b_{OHs}^{(3)}$	−31.017	192.23
$b_{OHp}^{(1)}$	1.5750	4.8613
$b_{OHp}^{(2)}$	−5.3854	−36.304
$b_{OHp}^{(3)}$	5.7422	148.70
$b_{OCs}^{(1)}$	3.1417	−2.4473
$b_{OCs}^{(2)}$	−72.970	5.3714
$b_{OCs}^{(3)}$	280.68	−2.5200
$b_{OCp}^{(1)}$	−1.4219	4.1875
$b_{OCp}^{(2)}$	0.68768	−14.753
$b_{OCp}^{(3)}$	34.603	14.290

C. Nonlinear minimization

Using the obtained parameters the total energy is now an analytic function of the atomic distances (and angles [8]), and it is used to calculate the PES. For the calculation, via this function, of the lowest-energy *path* (along a specified degree of freedom) or *surface* (in two specified degrees of freedom), and so on, we used a nonlinear energy minimization technique employing Powell's conjugate directions method [22] modified to be restricted to closed intervals of the DOF space [13].

TABLE IV. NRL coefficients of H-C TB Hamiltonian matrix elements in Eq. (6), in appropriate a.u.: The matrix element is measured in hartree and the distance in bohr; therefore, the NRL parameters $c^{(k)}$ are measured in hartree/bohr^k and g in bohr$^{-1/2}$. The first column refers to spin up and the second to spin down.

$c_{HCss\sigma}^{(0)}$	−173.11	12.718
$c_{HCss\sigma}^{(1)}$	175.83	−5.8982
$c_{HCss\sigma}^{(2)}$	−47.457	0.00406
$g_{HCss\sigma}$	1.4908	0.73061
$c_{HCsp\sigma}^{(0)}$	10.510	−23.762
$c_{HCsp\sigma}^{(1)}$	−8.4363	21.483
$c_{HCsp\sigma}^{(2)}$	2.4671	−6.3381
$g_{HCsp\sigma}$	1.0010	1.1310

TABLE V. NRL coefficients of H-O TB Hamiltonian matrix elements in Eq. (6) (in a.u., as in Table IV). The first column refers to spin up and the second to spin down.

$c_{HOss\sigma}^{(0)}$	−0.66732	−2.9258
$c_{HOss\sigma}^{(1)}$	0.50138	2.1864
$c_{HOss\sigma}^{(2)}$	0.05719	0.01801
$g_{HOss\sigma}$	0.40821	0.74185
$c_{HOsp\sigma}^{(0)}$	336.39	3.4677
$c_{HOsp\sigma}^{(1)}$	−325.06	−0.63940
$c_{HOsp\sigma}^{(2)}$	74.188	0.04553
$g_{HOsp\sigma}$	1.3829	0.22132

For comparison, each of the 724 *ab initio* CI calculations needs 3 h of CPU time on a HP-V2600 computer, each n-dimensional hypersphere radius r increase, to fit more remote points (with ten such hypersphere radial extensions all points can be covered) needs 2–3 h, while each two-dimensional energy minimization, using the final TB parameters (i.e., the lowest-energy path or surface determination), needs a few seconds.

III. RESULTS OF THE TB HAMILTONIAN FIT

A. The fit

Figure 1 shows that the TB Hamiltonian produces naturally the diabatically extended branch of the energy. Therefore, it can distinguish to which adiabatic state near an avoided crossing the CI values belong. (Classifying such CI points may sometimes be misleading if they are unrecognizable by mere observation of the MCSCF orbitals.) In Fig. 1,

TABLE VIII. NRL coefficients of H-O TB overlap matrix elements in Eq. (8) (in a.u., as in Table VII). The first column refers to spin up and the second to spin down.

$a_{HOss\sigma}$	0.36425	2.2057
$b_{HOss\sigma}$	0.21608	1.3084
$c_{HOss\sigma}$	0.0000	0.0000
$g_{HOss\sigma}$	1.1681	0.81240
$a_{HOsp\sigma}$	1.0161	13.898
$b_{HOsp\sigma}$	0.60281	−1.0125
$c_{HOsp\sigma}$	0.0000	−0.12999
$g_{HOsp\sigma}$	1.1126	0.60392

TABLE VI. NRL coefficients of C-O TB Hamiltonian matrix elements in Eq. (6) (in a.u., as in Table IV). The first column refers to spin up and the second to spin down.

$c^{(0)}_{COss\sigma}$	133.31	11.287
$c^{(1)}_{COss\sigma}$	−150.70	−10.992
$c^{(2)}_{COss\sigma}$	45.027	3.0274
$g_{COss\sigma}$	1.4932	1.1823
$c^{(0)}_{COsp\sigma}$	0.85555	156.17
$c^{(1)}_{COsp\sigma}$	−0.79537	−178.33
$c^{(2)}_{COsp\sigma}$	0.24774	44.889
$g_{COsp\sigma}$	0.77516	1.7896
$c^{(0)}_{COpp\sigma}$	1.9257	−0.84971
$c^{(1)}_{COpp\sigma}$	−1.0331	0.80194
$c^{(2)}_{COpp\sigma}$	0.15996	−0.18615
$g_{COpp\sigma}$	0.70303	0.81147
$c^{(0)}_{COpp\pi}$	1.8161	−0.24214
$c^{(1)}_{COpp\pi}$	−1.1755	0.20557
$c^{(2)}_{COpp\pi}$	0.20258	−0.05645
$g_{COpp\pi}$	0.71763	0.57821
$c^{(0)}_{COps\sigma}$	23.256	−5.5661
$c^{(1)}_{COps\sigma}$	−17.357	5.5604
$c^{(2)}_{COps\sigma}$	3.8753	−1.6245
$g_{COps\sigma}$	1.1145	1.1245

the diabatic character of the prediction is clearly displayed.

However, the most impressive aspect of the TB Hamiltonian method (absent in conventional fitting methods) was that it discovered, through the fit, that at some points of the fitted data base (about 10 in 700) the CI calculation had

TABLE VII. NRL coefficients of H-C TB overlap matrix elements in Eq. (8), in appropriate a.u.: The overlap matrix element is dimensionless; therefore, g is measured in bohr$^{1/2}$ and a,b,c are dimensionless. The first column refers to spin up and the second to spin down.

$a_{HCss\sigma}$	1.2111	1.6062
$b_{HCss\sigma}$	0.71845	0.95283
$c_{HCss\sigma}$	0.0000	0.0000
$g_{HCss\sigma}$	1.0254	0.76969
$a_{HCsp\sigma}$	0.85676	1.5816
$b_{HCsp\sigma}$	0.50824	0.93824
$c_{HCsp\sigma}$	0.0000	0.0000
$g_{HCsp\sigma}$	0.88780	0.85901

TABLE IX. NRL coefficients of C-O TB overlap matrix elements in Eq. (8) (in a.u., as in Table VII). The first column refers to spin up and the second to spin down.

$a_{COss\sigma}$	1.8859	1.2884
$b_{COss\sigma}$	0.71271	0.76434
$c_{COss\sigma}$	0.0000	0.0000
$g_{COss\sigma}$	0.91485	0.84572
$a_{COsp\sigma}$	1.1527	1.1257
$b_{COsp\sigma}$	0.68381	0.66782
$c_{COsp\sigma}$	0.0000	0.0000
$g_{COsp\sigma}$	0.79361	0.69786
$a_{COpp\sigma}$	1.0426	4.3592
$b_{COpp\sigma}$	0.61854	0.77345
$c_{COpp\sigma}$	0.0000	−0.08044
$g_{COpp\sigma}$	0.85808	0.93928
$a_{COpp\pi}$	0.98414	1.0268
$b_{COpp\pi}$	0.58381	0.60912
$c_{COpp\pi}$	0.0000	0.0000
$g_{COpp\pi}$	1.0624	1.0099
$a_{COps\sigma}$	1.1528	1.1411
$b_{COps\sigma}$	0.68389	0.67696
$c_{COps\sigma}$	0.0000	0.0000
$g_{COps\sigma}$	0.83985	0.94506

inadvertently converged to *excited* energies (which ought to be disregarded; otherwise, they would destroy the fit—whereas by a conventional method these would be erroneously fitted). Two examples are given: namely, points *A* and *B* in Figs. 2 and 3 for the fit of the first and second CI roots, respectively. Indeed we recalculated these points with special elaboration and found the correct states, but we stress that, *in practice*, among 700 calculation outcomes of comparable energy, 10 can hardly be *a priori* judged and disregarded as wrong, and if a conventional polynomial fit were used, these would be fitted, resulting to a wrong PES. Therefore, the TB Hamiltonian discovers any interpretation error, or failure, in a given fitting data base.

We approximate the adiabatic passing through a PES crossing by adopting the *lowest lying* of the two PES's at each side. For O-CH the two PES crossings occur at *large* separations from the absolute energy minimum and, there, the differences between the first and second roots are small; therefore, in approximating the adiabatic PES, we also fitted the first root everywhere (with the exceptions of the previous paragraph) by a single set of TB Hamiltonian parameters. These are displayed in Tables I–IX; the Hamiltonian and overlap matrix elements of similar atoms (100 a.u. apart) vanish. The total PES has at least five local minima H+C+O, HC+O, H+CO, C+HO, and HCO. These parameters refer to the last one.

B. Predictions

The fitted TB Hamiltonian could predict correctly total energy curves for points *not included* in the fit as shown for

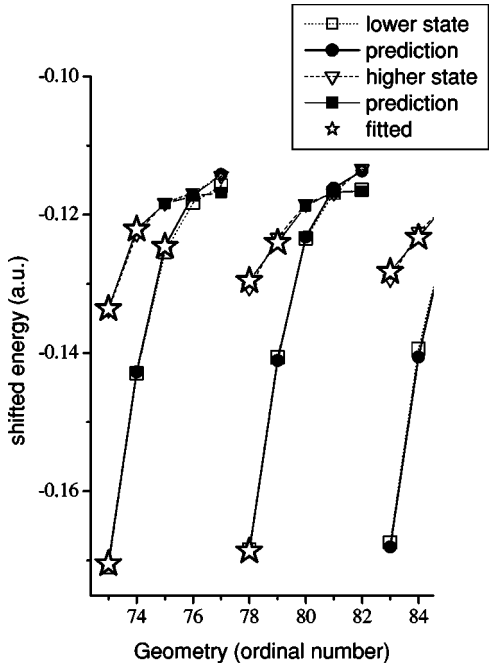

FIG. 1. Geometric structures indicated by open stars were included in the fits of the first and second CI roots. The horizontal axis refers to the ordinal number of the geometric structure in the CI database. The open squares and triangles are the original CI points. The solid circles and squares are predictions (not included in the fit). The TB Hamiltonian predicts the diabatic states: The squares of structures 77 and 82 belong to the lower-energy set, but clearly are diabatic continuations of the open triangle curves, which, before the crossing, belong to the higher-energy set and vice versa. The unbiased TB Hamiltonian fit predicts the diabatic continuation. A conventional fitting method could not recognize such crossings.

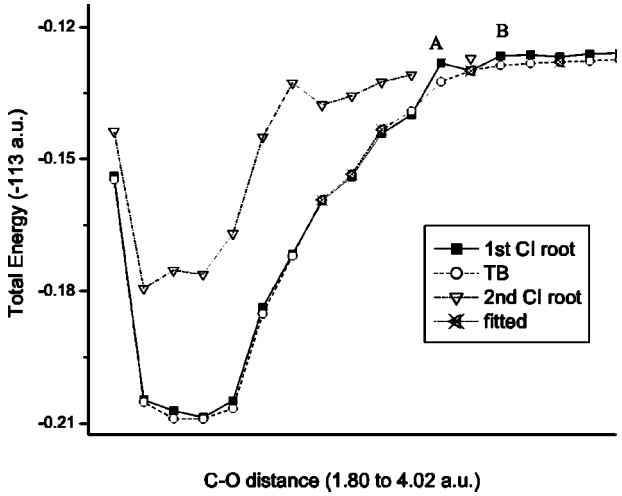

FIG. 2. TB Hamiltonian fit to the 1st CI root for H-C distance 2.1295 a.u., $\theta = 180°$. The CI points *A* and *B* are predicted to belong to the second root, as the TB Hamiltonian fit of the first CI root suggests to discard them. The TB Hamiltonian fit prompted our attention to look for the missing correct CI values. If the CI points were from a third party database, the *A* and *B* points should have to be disregarded, a recognition impossible by conventional fitting methods. The meaning of the horizontal axis is as in Fig. 1. It is remarkable that the seven leftmost TB points "in the well," although not fitted, coincide with the CI values.

example in Figs. 4 and 5 for various cases. The comparison between the predicted energy points and the (not fitted) *ab initio* CI points is excellent, comparable to that of the fitted. In both fitted and predicted points the differences between the *ab initio* CI energies and the TB Hamiltonian total energies are less than 0.6 kcal/mol. These, representing differences between two smooth surfaces, are systematically (not randomly) distributed, as seen, for example, in Fig. 6, which is identical in context with Fig. 2, except that the horizontal axis represents the *actual* C-O distance (in a.u.), instead of the geometric structure count. Because of this, the aforementioned in Fig. 2 (excited) points *A* and *B* are not clearly distinguishable from the nearby database points. It is remarkable that the seven leftmost TB points (around the minimum), although not fitted, are predicted to coincide with the CI values within the fitting error.

1. Lowest-energy path

Using the fit, we calculated the minimum-energy path for the formation of HCO, as HC approaches O, shown in Fig. 7. For a triatomic molecule the figure contains the whole information: As CH approaches O, for every O-C distance the *minimum energy with respect to the O-C-H angle* is found and displayed. At each O-C calculated point the orientation of CH with respect to the (horizontal) O-C orientation is

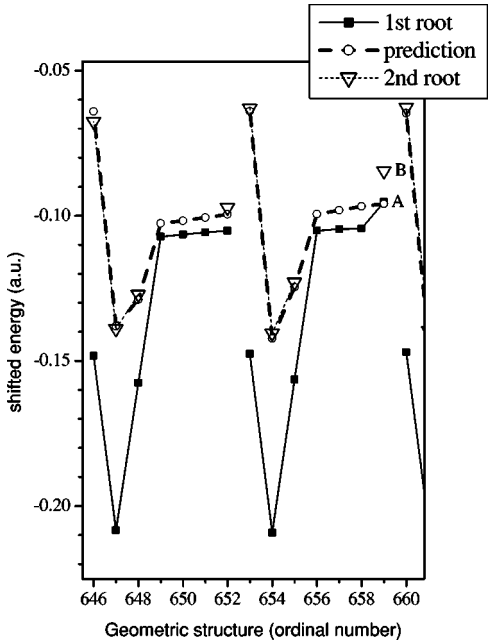

FIG. 3. TB Hamiltonian fit to the second CI root. The first three points of each curve were fitted. Nonfitted open circles are predictions. As in Fig. 2, in the second curve the fit predicts that the CI points *A* and *B* of structure 659 actually belonged to the second and third roots, respectively, to which the MCSCF iterative procedure had originally converged, missing the first root. The TB Hamiltonian fit prompted attention to look for the missing CI root. A conventional fitting method could not recognize that point *A* of the database belongs to the second root and that point *B* should be entirely aborted. The meaning of the horizontal axis is as in Fig. 1.

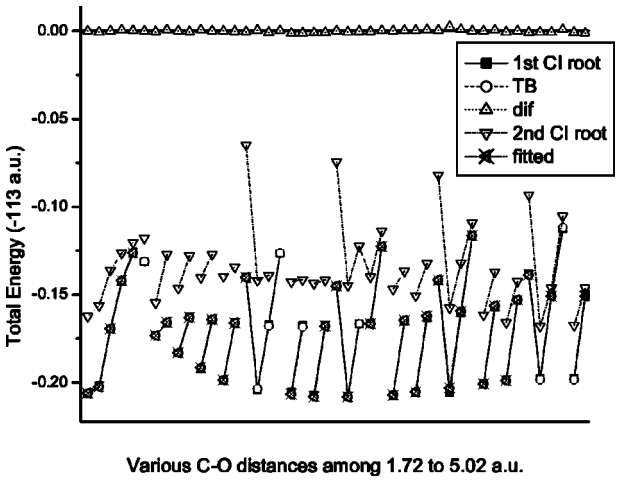

FIG. 4. Comparison of the TB predicted to the corresponding CI not fitted total energy E in a.u. for C-H distance=3.01 a.u. Several (connected) E vs C-O distance curves are shown, each for a different HCO angle between 50° and 180°. The fitted CI points are indicated by asterisks, the predicted by open circles, and the differences by upper triangles. The black squares represent the original CI energies of the lowest state (first root) and the down triangles of the second root. In both fitted and predicted points the differences between the *ab initio* CI energies and the TB Hamiltonian total energies (upper triangles) are less than 0.6 kcal/mol. The meaning of the horizontal axis is as in Fig. 1.

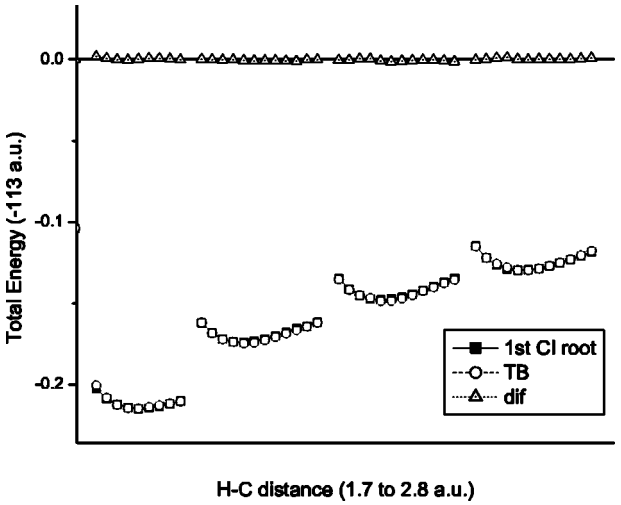

FIG. 5. Comparison of the TB predicted to the corresponding CI not fitted total energy E in a.u. for HCO angle=100°. Four (connected) E vs C-H distance curves are shown, each for a different C-O distance. The first, third, and fourth sets (curves) from the left, for C-O distances 2.5, a.u., 3.8 a.u., and 4.8 a.u., respectively, were fitted; the second (C-O=3.2 a.u.) is entirely predicted and coincides with the corresponding *ab initio* CI, but not fitted, set. The black squares represent the original CI energies of the lowest state (first root). In both fitted and predicted points the differences between the *ab initio* CI energies and the TB Hamiltonian total energies (upper triangles) are less than 0.6 kcal/mol. The meaning of the horizontal axis is as in Fig. 1.

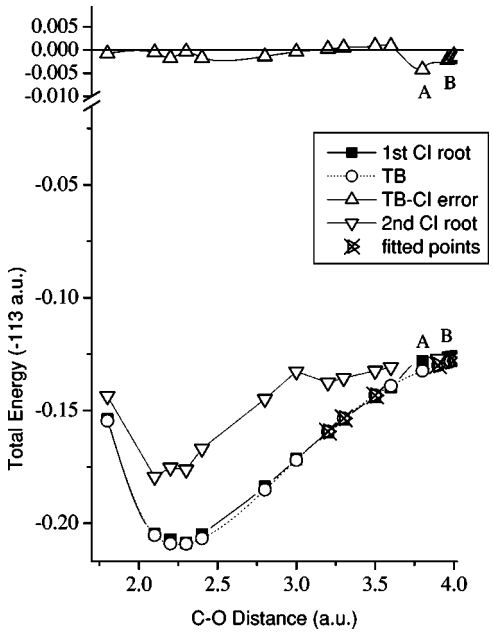

FIG. 6. The fitting error shows a systematic (not random) smooth distribution along the PES, due to the differences between two smooth surfaces—i.e., that of of TB and CI—as shown, for example, in the same to Fig. 2 subset of the CI and TB values, but as a function of the *actual* C-O distance (not the structure ordinal number). In this scale points *A* and *B* are close to nearby database points, therefore, not clearly distinguishable.

also indicated by an arrow originating from C (displayed *on* the energy curve) and ending at H. Thus, as CH starts sliding down the minimum energy "potential well," at large distances H is bent toward O, but as CH approaches O, gradually H bends away from O. At equilibrium the O-C-H angle is 121.417° corresponding to a prediction for the *CI value*. The SCF value was 126°, and other values (cf. [23] and references therein) are theoretical, 128° and 130°, and experimental, 120°, 123.8°, 125°, and 127.426°. The corresponding CH and CO distances are calculated as 2.097 and 2.246 a.u., respectively. To our knowledge, there is no experimental confirmation of the lowest-energy path of this intermediate molecule. The TB Hamiltonian fit predicts an *antisymmetric stretching* vibration around C near equilibrium: As seen in Table X, around equilibrium the angle does not change appreciably, but the C-H distance increases slightly as the O-C distance decreases.

2. Lowest-energy surface

Figure 8 shows the TB PES of O in the vicinity of HC, for which the fit was performed, restricted at C-H distance of 2.1295 a.u. for various C-O distances and H-C-O angles around the HC-O equilibrium geometry. The corresponding *ab initio* CI points (either fitted or not) are shown on the surface. Angles smaller than 50°, corresponding to large interaction of H with O, as well as points at large C-H distances, outside the vicinity of HC (+O), rather corresponding to the vicinity of CO (+H), were not fitted. For the PES under examination (of O in the vicinity of CH) we computed on a regular mesh of H-C-O angles and C-O separations,

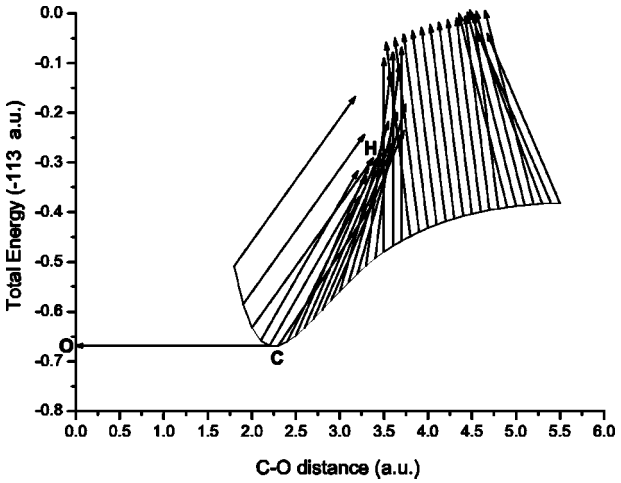

FIG. 7. The TB minimum energy path for the system of HC +O. For each O-C distance the TB energy was minimized (i.e., searched for minimum) with respect to the C-H distance and O-C-H angle. The minimum energy and the corresponding C-H distance and O-C-H angle are displayed as follows: If C is considered on the energy curve and O on the energy axis keeping the $\vec{CO}$ arrow horizontal, then the $\vec{CH}$ arrow indicates the position of H relative to the C and O. At large O-C distances, CH is bent toward O, the O-C-H angle gradually becoming 121.417°. The displayed data are entirely interpolated predictions based on the TB parameters. There were no *ab initio* CI points to be fitted on this curve, since the *optimal* values (minima), used to produce the curve, were unknown before the optimization.

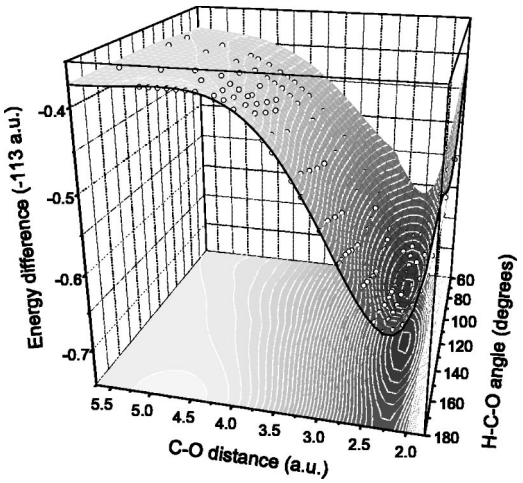

FIG. 8. TB Hamiltonian prediction of the HC-O PES at C-H distance of 2.1295 a.u. for various C-O distances and H-C-O angles around the HC-O equilibrium geometry, for which the fit was performed. The corresponding *ab initio* CI points (either fitted or not) are shown on the surface. Angles smaller than 50° corresponding to H-CO were not fitted.

the lowest TB energy surface for the optimized (minimizing the TB energy) C-H distance. In the resulting two-dimensional surface (Fig. 9) the optimal C-H distance (yielding the lowest energy) is not seen. The two-dimensional surface indicates the existence, besides the main, of two more energy minima, both in linear geometry of 0° and 180°. However, because there are no CI points near there, these energy minima, being far away from the region of the fit, are unreliable and should be considered as areas of interest to be checked and corrected with corresponding CI points. Indeed, it is known that the HCO surface has two relatively low- energy cusps at linear geometries, one for H approaching CO and one for aproaqching OC. These cuspe result from the crossing of $^2\Sigma$ and $^2\Pi$ electronic states, which

TABLE X. Geometric characteristics of HC-O around equilibrium, along the minimum-energy path, in a.u. (H-C-O angle in degrees). For each CO distance the TB Hamiltonian energy minimum is searched in the space of the remaining degrees of freedom: HC distance and H-C-O angle. The last three columns indicate the minimum energy molecular geometry. Around equilibrium the angle changes slightly monotonically by 1°–2°, but because the C-H distance decreases as the O-C distance increases, predominantly an *antisymmetric stretching* vibration occurs.

C-O distance	Total energy	C-H distance	H-C-O angle
2.6	−113.6328	2.069	117.53
2.5	−113.6485	2.071	118.69
2.4	−113.6610	2.077	119.77
2.3	−113.6685	2.088	120.84
2.2	−113.6687	2.107	121.91
2.1	−113.6583	2.130	122.98
2.0	−113.6326	2.153	124.09

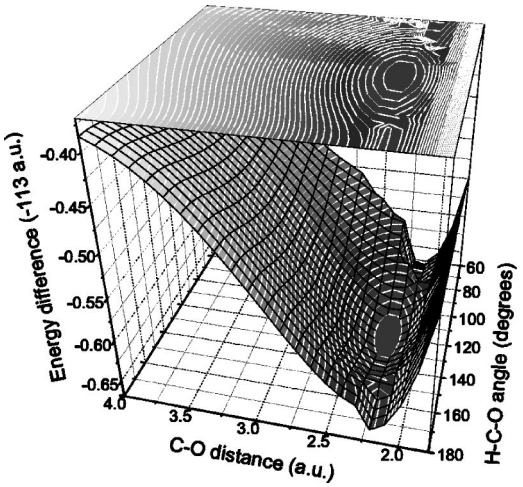

FIG. 9. TB Hamiltonian prediction of the HC-O PES, as in Fig. 8, but with *optimized* (lowest energy) C-H distance. On a regular mesh of C-O distances and H-C-O angles, a minimization of the TB total energy were performed with respect to the C-H distance, and the optimal energy is displayed (vertical axis). There are no *ab initio* CI points on this surface, since the *optimal* C-H distance, used to produce the surface, was unknown in advance. Therefore, this PES is an interpolating prediction based on the TB parameters fitting the existing CI database. The TB Hamiltonian clearly predicts the existence of three energy minima, the main at 121.417°, and two higher lying, corresponding to the linear H-CO or C-OH, as explained in the text.

becomes an avoided crossing in nonlinear geometries [12,23]. Their thorough examination and possible creation of relevant parameters for these regions is beyond the scope of this fitting demonstration.

3. Normal-mode frequencies

The first CI root energy minimum (ground-state equilibrium) occurs at the internal coordinates $r_{CH}=2.09722$ a.u., $r_{CO}=2.24596$, and $\theta_{H\text{-}C\text{-}O}=121.41°$. With the analytic TB Hamiltonian fit, it is trivial to calculate the PES curvatures at equilibrium in terms of these internal coordinates and the corresponding normal-mode frequencies. These are obtained almost decoupled to pure H-C-O bending, C-O stretching, and C-H stretching with eigenfrequencies (and corresponding eigenvectors) $\nu_1=1093.64\ \mathrm{cm}^{-1}$ $(0.012r_{CH},\ 0.014r_{CO},\ 0.999\theta)$, $\nu_2=1848.73\ \mathrm{cm}^{-1}$ $(-0.122r_{CH},\ 0.959r_{CO},\ -0.256\theta)$, and $\nu_3=3052.19\ \mathrm{cm}^{-1}$ $(0.999r_{CH},\ -0.023r_{CO},\ -0.037\theta)$. The experimental values are $\nu_1=1080.76\ \mathrm{cm}^{-1}$, $\nu_2=1868.17\ \mathrm{cm}^{-1}$, and $\nu_3=2434.48\ \mathrm{cm}^{-1}$, respectively [24]. The classical frequency of the C-H stretching was found to be larger than the experimental value. The agreement with the other experimental values is quite reasonable. The same frequencies can be obtained by calculating the curvature along the internal coordinate "directions" r_{CH}, r_{CO}, and $\theta_{H\text{-}C\text{-}O}$, achieved by straightforward minimization (i.e., locating the minimum) of the TB Hamiltonian energy at a dense mesh along the desired "direction." Since the TB Hamiltonian bonding matrix elements of H-C and H-O are appreciable, we also calculated the minimum TB Hamiltonian energy (and the curvature) along the direction from H toward the center of mass of C and O. The frequency along this direction is $\nu=2208.3\ \mathrm{cm}^{-1}$ Bownman *et al.* [12] had computed the normal-mode frequencies with a smaller basis set, and about 12 000 configurations, to $\nu_1=1156\ \mathrm{cm}^{-1}$, $\nu_2=1903\ \mathrm{cm}^{-1}$, and $\nu_3=2815\ \mathrm{cm}^{-1}$; our better agreement with experiment is attributed to the higher accuracy of our CI calculations (and, of course, to the accurate fit).

IV. CONCLUSIONS

The TB Hamiltonian fitting to *ab initio* CI energies is a promising method of natural interpolation. It has the advantages that it is analytic and quick, it needs relatively few CI energies to be fitted, not necessarily on a regular mesh, and can serve as a guide to *decide* whether in a given fitting data base each point belongs to the desired PES—an impossible feature with standard polynomial interpolation methods. It has the disadvantage—common to all interpolation schemes—that it cannot be used reliably to extrapolate far away from the region of the fit. However, even then, it can locate candidate features of the PES to be checked and corrected with further appropriate CI points.

ACKNOWLEDGMENT

We wish to thank Dr. M. J. Mehl for many useful discussions.

[1] Y.-S. M. Wu, A. Kuppermann, and J. B. Anderson, Phys. Chem. Chem. Phys. **1**, 929 (1999).
[2] R. McWeeny, J. Mol. Struct.: THEOCHEM **261**, 403 (1992); N. C. Bacalis, Chem. Phys. Lett. **331**, 323 (2000) and references therein.
[3] P. Hohenberg and W. Kohn, Phys. Rev. **136**, B864 (1964); W. Kohn and L. J. Sham, Phys. Rev. **140**, A1133 (1965); **145**, A561 (1966); U. von Barth and L. Hedin, J. Phys. C **5**, 1629 (1972).
[4] Y. Yourdshahyan, B. Razaznejad, and B. I. Lundqvist, Phys. Rev. B **65**, 075416 (2002).
[5] J. N. Murrell, S. Carter, S. C. Farantos, P. Huxley, and A. J. C. Varandas, *Molecular Potential Energy Functions* (Wiley-Interscience, New York, 1984).
[6] N. C. Bacalis, D. A. Papaconstantopoulos, M. J. Mehl, and M. Lach-hab, Physica B **296**, 125 (2001).
[7] D. A. Papaconstantopoulos and M. J. Mehl, J. Phys.: Condens. Matter **15**, R413 (2003).
[8] J. C. Slater and G. F. Koster, Phys. Rev. **94**, 1498 (1954).
[9] The *ab initio* CI energies were computed by MOLPRO, a package of *ab initio* programs written by H.-J. Werner and P. J. Knowles, with contributions from J. Amlöf *et al.*
[10] C. Vinckier, M. P. Gardner, and K. D. Bayes, J. Chem. Phys. **81**, 2137 (1977); M. P. Gardner, C. Vinckier, and K. D. Bayes, Chem. Phys. Lett. **31**, 318 (1975).
[11] A. Metropoulos and A. Mavridis, J. Chem. Phys. **115**, 6946 (2001).
[12] J. M. Bowman, J. S. Bittman, and L. B. Harding, J. Chem. Phys. **85**, 911 (1986).
[13] N. C. Bacalis, J. Phys. B **29**, 1587 (1996).
[14] T. H. Dunning, Jr., J. Chem. Phys. **90**, 1007 (1989).
[15] A. K. Wilson, T. V. Maurjk, and T. H. Dunning, Jr., J. Mol. Struct.: THEOCHEM **388**, 339 (1997).
[16] C. W. Misner, K. S. Thorne, and J. A. Wheeler, *Gravitation* (Freeman, San Francisco, 1973).
[17] M. J. Gillan, J. Phys.: Condens. Matter **1**, 689 (1989).
[18] J. Pople and D. Beveridge, *Approximate Molecular Orbital Theory* (McGraw-Hill, New York, 1970).
[19] R. Daudel, G. Leroy, D. Peeters, and M. Sana, *Quantum Chemistry* (Wiley-Interscience, New York, 1983).
[20] R. Hoffmann, J. Chem. Phys. **39**, 1397 (1963); E. Hückel, Z. Phys. **70**, 204 (1931); **76**, 628 (1932).
[21] M. J. Mehl and D. A. Papaconstantopoulos, Phys. Rev. B **54**, 4519 (1996).
[22] W. H. Press, S. A. Teukolsky, W. T. Vetterling, and B. P. Flannery, *Numerical Recipes in FORTRAN*, 2nd ed. (Cambridge University Press, Cambridge, England, 1992).
[23] P. J. Bruna, R. J. Buenker, and S. D. Peyerimhoff, J. Mol. Struct. **32**, 217 (1976); H. Y. Wang, J. A. Eyre, and L. M. Dorfman, J. Chem. Phys. **59**, 5199 (1973).
[24] J. D. Tobiason, J. R. Dunlop, and E. A. Rohlfing, J. Chem. Phys. **103**, 1448 (1995); M. E. Jacox, NIST Vibrational and Electronic Energy Levels Database, Version 3.0, NIST, Washington, D.C., 1993, and references therein.